Letter

Studying Edge Defects of Hexagonal Boron Nitride Using High-Resolution Electron Energy Loss Spectroscopy

Chang Tai Nai,[†,‡] Jiong Lu,[†] Kai Zhang,[†] and Kian Ping Loh*,[†]

[†]Department of Chemistry and Graphene Research Centre, National University of Singapore, 3 Science Drive 3, Singapore 117543
[‡]NUS Graduate School for Integrative Sciences and Engineering, National University of Singapore, Centre for Life Sciences, #05-01, 28 Medical Drive, Singapore 117456

S *Supporting Information*

ABSTRACT: Studying the phonons of hexagonal boron nitride (h-BN) is important for understanding its thermal, electronic, and imaging applications. Herein, we applied high-resolution electron energy loss spectroscopy (HREELS) to monitor the presence of edge defects in h-BN films. We observed an edge phonon at 90.5 meV with the initial formation of island-like domains on Ru(0001), which subsequently weakens with respect to the bulk phonon as the islands congregate into a film. The presence of a weak edge phonon peak even at full surface coverage of the h-BN film indicates the sensitivity of HREELS in detecting line defects. A shoulder peak at ∼160 meV assignable to sp^3 bonded modes was attributed to grain boundaries arising from misaligned domains. In addition, the strengths of substrate interaction and the rippling of the h-BN film can be judged from the shift in the phonon energy of the out-of-plane $TO_\perp$ mode.
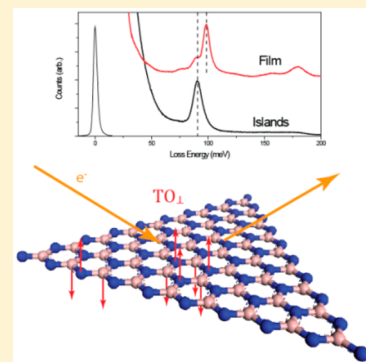
Hexagonal boron nitride (h-BN) is a van der Waals material that can exist as a 2D crystal with a hexagonal structure similar to graphene but with a boron–nitrogen pair in its unit cell. The structural similarity to graphene imparts h-BN with comparable structure-based properties, such as a high thermal conductivity,[1] but the difference in composition causes it to be an insulator with a bandgap of 6 eV,[2] and thus h-BN can be used as an ultrathin dielectric material with good heat-dissipation properties.[3]

Phonons are lattice vibrations where neighboring atoms oscillate in specific directions depending on the specific phonon mode and are the primary mechanism in thermal conduction. The interactions between phonons and other particles are widely studied for their impact on applications, such as scattering interactions that affect thermal transport[4] and electron mobility[5,6] and coupling with infrared photons to form phonon polaritons,[7] which show potential for imaging and detection applications.[8]

Because phonons are lattice vibrations, they are sensitive to anomalies in the periodicity of the lattice, such as defects, grain boundaries, and edges. In particular, localized edge effects on phonons are interesting due to the abundance of edges in nanosized materials.[9] Such edge-localized phonons have been observed in graphene to impact thermal transport[10] and conductance,[11] demonstrating their importance in applications; however, there is a lack of detailed studies on the edge phonons of h-BN. Raman scattering is frequently used to characterize 2D films, such as monolayer graphene and monolayer h-BN.[12] Although h-BN has two Raman active modes, only the high-energy mode can be detected experimentally as the lower

energy mode falls below the typical cutoff energy in Raman scattering.

High-resolution electron energy loss spectroscopy (HREELS) is a surface-sensitive technique that probes the low-energy vibrational modes through scattering of incident electrons. Specular scattering in HREELS is dominated by the mechanism of dipole scattering, where the incident electron interacts with an oscillating dipole. The two-atom unit cell of monolayer h-BN results in six phonon modes: three acoustic and three optical phonons. The polar nature of B–N bonds leads to oscillating dipoles in the optical phonon modes, making them easily detectable by specular HREELS, in contrast with Raman scattering. The three optical phonons are identified by their oscillation direction, namely, the out-of-plane transverse phonon ($TO_\perp$), the in-plane transverse phonon ($TO_\parallel$), and the longitudinal phonon (LO). Because of the orientation of the $TO_\perp$ mode and the selection rule of HREELS for vibrations with dipole moments normal to the surface, this mode is strong and can be easily seen in the spectrum, in contrast with the other two in-plane modes.

To investigate the edge effect on phonon energies of monolayer h-BN, we studied monolayer h-BN in different stages of its film growth, that is, from islands to a completely coalesced film. h-BN was grown by the thermal decomposition of borazine ($B_3N_3H_6$) on Ru(0001), as had been demonstrated in previous STM studies.[13,14] Ru(0001) has an in-plane lattice constant of 2.71 Å, which is a 8.4% mismatch with that of h-BN

(lattice constant 2.50 Å), resulting in an incommensurate structure; however, besides the lattice constant, the strength of the interactions between the close-packed metal surface with the h-BN layer also plays an important role in the formation of moiré superstructure. Compared with other metal surfaces that form incommensurate structures with h-BN, such as Pt(111) and Pd(111) (lattice constants 2.78 and 2.75 Å, respectively), the lesser filled d orbitals of Ru leads to a higher binding energy with the h-BN layer,[15] resulting in a highly corrugated moiré pattern known as h-BN nanomesh.[14] While HREELS had been performed on commensurate h-BN layers on Ni(111) surface[16] and incommensurate, weakly physisorbed h-BN layers on Pt(111) and Pd(111) surfaces,[16,17] no studies have been carried out on incommensurate, strongly bound h-BN nanomesh on Ru(0001) surface, where the strong metal−BN interaction can be expected to have an impact on the phonon energies. To probe the effect of the substrate on the phonons of h-BN, we carried out similar growth on polycrystalline Pt foil for comparison.

Figure 1 shows the STM image of monolayer h-BN grown on Ru(0001). The images reveal that in the initial stage of the
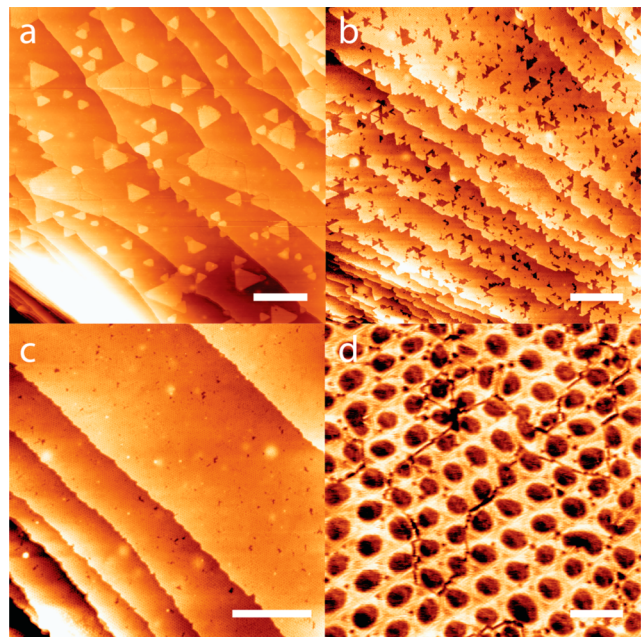

Figure 1. STM images of h-BN grown on Ru(0001), showing the evolution of the structure of monolayer h-BN from (a) triangular islands, to (b) a coalescing film, to (c) a near complete film. (d) Magnified image of the film in panel c shows distinctive moiré pattern and line defects. Scale bars are (a−c) 100 and (d) 5 nm, respectively.

growth, the surface of Ru(0001) is dotted with triangular "islands" of h-BN (Figure 1a). Triangular h-BN islands with one single type of edge are dominant due to the relative stability of the N-terminated edges over the B-terminated edges.[13,18] An increase in the dosage of borazine leads to the merging of the islands (Figure 1b) to form a near complete film (Figure 1c). The presence of the h-BN film is manifested by a distinctive "nanomesh" moiré pattern formed by the incommensurate lattices between h-BN and the Ru surface (Figure 1d), which was first reported on Rh(111).[19] Ab initio calculations suggested that this pattern is a result of strong binding energy between the h-BN layer and the metal substrate.[15] Among the close-packed metal surfaces used to

grow h-BN, Ru(0001) has the highest binding energy, and the resultant film has the largest corrugation.[20] In contrast, h-BN film interacts less strongly with a Pt(111) surface, giving a relatively flat moiré pattern.[21] The magnified image also reveals the presence of several line defects on the monolayer h-BN film. These are due to misfit grain boundaries arising from the heteronuclear nature of h-BN and the incompatibility of N−N bonds and B−B bonds. Hence, two independently grown islands may not be able to meet at the correct position to enable them to fuse together, leaving behind a gap where the grain boundary should be. It is interesting to see if HREELS will be sensitive to the presence of these line and edge defects as well as ripples in the films.

Figure 2a shows the specular HREEL spectra of monolayer h-BN films prepared using different dosages of borazine. The spectra clearly show the peaks that correspond to the optical phonon modes of h-BN, in particular, a very strong peak between 90−100 meV. Off specular HREELS demonstrates that this strong peak decreases in intensity much more significantly compared with the other peaks at 180 meV (Figure 2b), indicating strong dipole scattering contribution characteristic of out-of-plane vibrations. This confirms the assignment of the strong peak to the out-of-plane $TO_\perp$ mode and the other impact scattered peaks to the in-plane modes.

From the HREEL spectra, it is clear that the $TO_\perp$ peak is sensitive to the morphology of the film. In the initial stages of film growth, where h-BN islands are formed, the $TO_\perp$ peak is ∼90.5 meV, which is significantly lower than several other reported values on various metal surfaces;[16] however, when the coverage of the h-BN film increases, a shoulder starts to appear at 98 meV, which grows stronger and eventually dominates the spectrum.

These changes in the phonon peak positions reflect transition of the h-BN film from an island stage to a complete film. The lower energy $TO_\perp$ peak in the island stage can be attributed to the edge atoms on the h-BN islands. To stabilize the edges, the atoms may undergo some form of reconstruction or form strong bonds with the underlying substrate to stabilize themselves. The result is a shift in the phonon energy from that of the bulk atoms, creating the edge phonons.[9] Similar lower energy phonon peaks have been reported when h-BN films were broken up by heating[22] and during the initial growth of monolayer h-BN on Pt(111) surface.[17]

In a continuous film, the effects of such edge states are much less significant. The film samples primarily show a $TO_\perp$ phonon energy (98 meV), which is close to that reported on other incommensurate metal surfaces, such as Pt and Pd.[16] HREELS appear to be particularly sensitive to line defects remaining in the film because the presence of a weak edge phonon peak can be detected even at full surface coverage of the h-BN film.

The in-plane phonon modes ($TO_\parallel$ and LO) also show a trend with respect to the different stages of h-BN growth (Figure 2a). During the low dosage phase, almost no peaks can be observed in this region, and only a very weak peak may be observed at 180 meV; however, when the islands start to coalesce, a broad peak can be observed to increase gradually at 179 meV. This peak is likely a composite peak of both in-plane phonon modes, which are expected to overlap between 170 to 183 meV.[16] The gradual appearance of the in-plane modes as the h-BN islands grow into a film could be due to the rippling of the h-BN monolayer, as it forms a moiré pattern on Ru(0001) under compressive strain, causing the in-plane
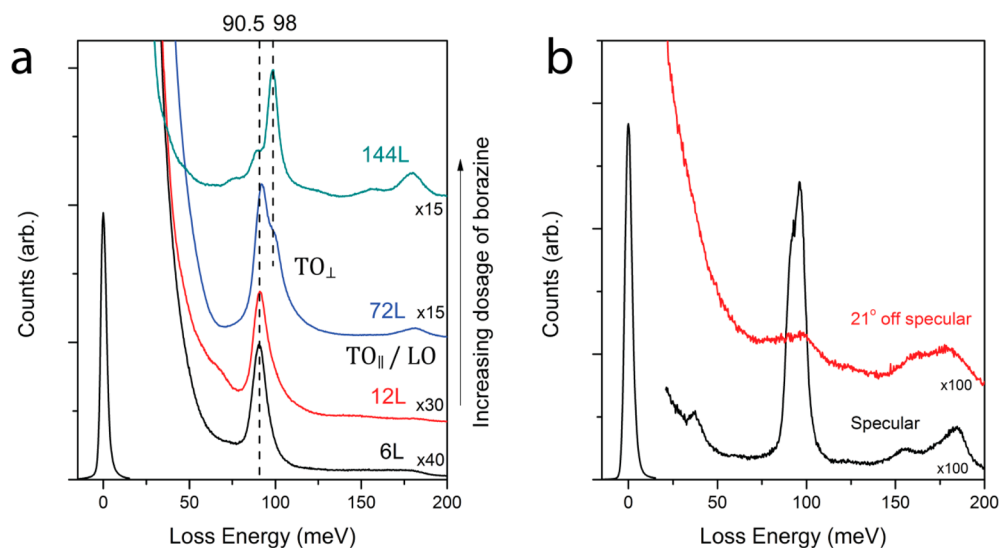
Figure 2. (a) HREEL spectra of h-BN grown on Ru(0001) using different dosages of borazine (6−144 L) and (b) measured in the specular direction and 21° off specular direction.

vibration vector to be no longer strictly parallel to the surface, thus allowing weak excitation of the in-plane modes.

Interestingly, as the h-BN film grows, a shoulder could be observed to appear at ∼158 meV, which does not match any known in-plane phonon mode energy and was not observed in HREELS of complete h-BN film on other metal surfaces.[16] One possible reason for this peak is the presence of some sp^3 character in the h-BN film. Cubic BN, an sp^3 allotrope of BN, has optical phonons at approximately 130 and 160 meV.[23] The lack of a peak at 130 meV indicates that the film consists of majority sp^2 bonded phase, but a broad in-plane modes peak and the shoulder peak suggest that there is some degree of sp^3 hybridization.[24] This sp^3 character may be manifested at the grain boundaries of the h-BN film that are formed when the islands merge, which explains its gradual increase in intensity as the film grows.

Figure 3 shows the specular HREEL spectra obtained when similar growth conditions were performed on Pt foil. The $TO_\perp$

peak for the h-BN film agrees with the reported value for h-BN film on Pt(111) surface (99 meV);[16,17] however, the in-plane modes form a very strong and broad peak at 182 meV, possibly due to the formation of a disordered h-BN film on the rough and polycrystalline surface of the platinum foil. Similar to the h-BN film on Ru(0001), a shoulder at ∼161 meV indicates the presence of some sp^3 character.

However, unlike the Ru(0001) surface, h-BN islands on Pt foil (2.4 L) show a $TO_\perp$ peak at 98 meV. This is in contrast with the observation on Pt(111), where a lower energy peak at 93 meV is observed during the growth process.[17] This is probably due to the random grain orientation of the polycrystalline Pt foil, which results in misalignment between the h-BN lattice and the substrate, negatively impacting the interaction between the edge atoms and the underlying substrate, resulting in an overall weaker interaction and a higher phonon energy.

A comparison of the $TO_\perp$ peak position of monolayer h-BN islands or film deposited on the different substrates can be seen in Figure 4, and a summary of the peak positions for all the h-BN optical phonons is listed in Table 1. The result suggests a softening of the phonon mode with stronger interaction between substrate and h-BN film. From the Figure and the Table, it can be observed that $TO_\perp$ peak position is higher for Pt foil surface compared with the Ru(0001) and highest for free-standing h-BN film. A similar trend can be seen in the in-plane phonon modes, even though the peak could not be resolved into the individual modes as well as in the sp^3 related mode at ∼160 meV. The $TO_\perp$ peak position for the free-standing h-BN film is the closest to that for exfoliated h-BN nanosheets[25] and CVD grown h-BN thin films.[26,27]

The softening effect has been reported on Ni(111), on which h-BN forms a commensurate layer, resulting in a π−d orbital hybridization that downshifts the $TO_\perp$ phonon significantly.[16] Although the $TO_\perp$ peak positions of h-BN film on Ru(0001) and Pt foil are slightly softened compared with bulk h-BN, the amount of softening is very small, suggesting that the overall h-BN-substrate interaction is not very strong, as both metals form incommensurate structures with h-BN. However, the larger softening of the $TO_\perp$ phonon on Ru(0001) reflects a stronger interaction of h-BN with single crystalline Ru compared with
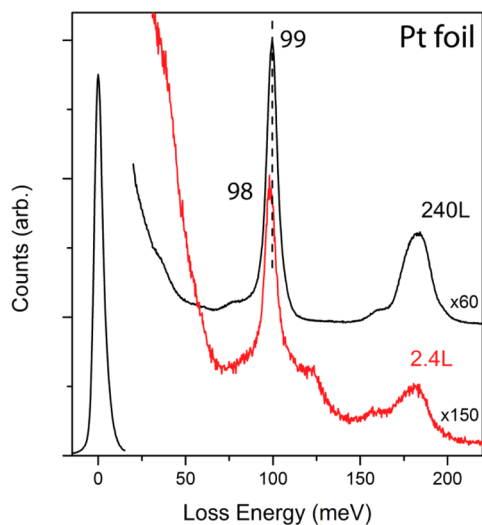

Figure 3. HREEL spectra of h-BN grown on Pt foil for low (2.4 L) and high (240 L) borazine dosages corresponding to islands and films, respectively.
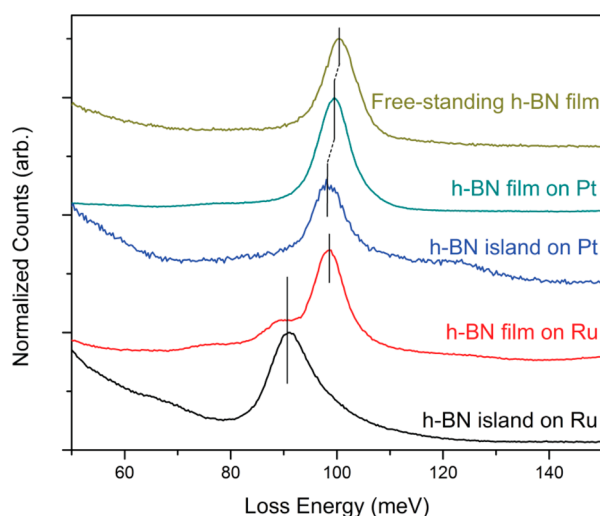
Figure 4. Comparison of the TO$_\perp$ peak of various monolayer h-BN samples grown on different substrates and under different conditions. The spectra are normalized to the maxima of the respective TO$_\perp$ peaks.

polycrystalline Pt foil, which agrees with theoretical calculations[15] and the trend in the moiré pattern observed under STM.[20] This lends support to the possibility that the edges of the h-BN islands are stabilized by the stronger interaction with the Ru(0001) surface, leading to the large decrease in energy of the TO$_\perp$ phonon. Further theoretical studies will be required to shed more light on the phenomenon.

In summary, the phonon modes in h-BN, as detected by HREELS, are highly sensitive to the morphology, edge defects, and substrate interactions in h-BN. In particular, a highly softened TO$_\perp$ mode was observed for low coverage of h-BN on Ru(0001) that could be attributed to edge states of the triangular h-BN islands. The presence of line defects and grain boundaries can be detected by the presence of phonon modes at 90.5 and ~160 meV. In addition, the interaction between the h-BN lattice and the underlying substrate surface was found to influence the phonon energies of monolayer h-BN. These results highlight that edge and substrate effects are important considerations in applications of h-BN that involve phonon interactions, such as thermal dissipation and as a dielectric in electronic applications.

■ EXPERIMENTAL SECTION

Preparation of Monolayer h-BN. Borazine (B$_3$N$_3$H$_6$) is used as a precursor to grow monolayer h-BN films onto single crystal Ru(0001) surface (MaTek) in a UHV chamber. The Ru(0001) surface was first cleaned by repeated cycles of annealing in an oxygen atmosphere (5 × 10^{-8} mbar, 1073 K) and argon ion sputtering (4 × 10^{-5} mbar backfill, 1.8 kV) followed up by a flash anneal to 1273 K to remove surface oxygen. Borazine is passed into a preparation chamber with a base pressure of 8 × 10^{-10} mbar through a leak valve, while simultaneously heating the clean Ru(0001) single crystal through electron beam bombardment to 1173 K. The same growth procedure was also performed on Pt foil (Alfa Aesar). Free-standing monolayer h-BN film was prepared by transferring a h-BN film on Pt foil using PMMA onto a graphene film on Cu foil, followed by washing with acetone and annealing in vacuum.

Scanning Tunnelling Microscopy. STM measurements were performed in an ultrahigh vacuum chamber with a base pressure of 1.5 × 10^{-10} mbar. The chamber is equipped with an STM 150 Aarhus unit (SPECS) with the Nanonis (SPECS) SPM control system. The sample is typically prepared in the adjacent preparation chamber, then transferred to the STM unit and measured at 298 K.

High-Resolution Electron Energy Loss Spectroscopy. HREELS is performed using a Delta 0.5 spectrometer (SPECS) in a UHV chamber with a base pressure of 2 × 10^{-10} Torr. An incident electron energy of 5 eV is used. For general scans of the phonons, the scattered electrons are collected at the specular angle. Off specular measurements are performed by rotating the analyzer and detector with respect to the spectrometer axis.

■ ASSOCIATED CONTENT

ⓢ Supporting Information

The Supporting Information is available free of charge on the ACS Publications website at DOI: 10.1021/acs.jpclett.5b01900.

Additional names in references. (PDF)

■ AUTHOR INFORMATION

Corresponding Author
*E-mail: chmlohkp@nus.edu.sg.

Notes
The authors declare no competing financial interest.

Table 1. Summary of Phonon Peak Energies of h-BN on the Various Systems Determined with Specular HREELS in This Work, in Comparison with Literature Values Reported for Other Systems

system	surface structure	TO$_\perp$ (meV)	TO$_\parallel$ (meV)	LO (meV)	ref
h-BN islands/Ru(0001)	incommensurate	90.5	180[a]	180[a]	[b]
h-BN film/Ru(0001)	incommensurate	90, 98	179[a]	179[a]	[b]
h-BN islands/Pt foil	incommensurate	98	181[a]	181[a]	[b]
h-BN film/Pt foil	incommensurate	99	182[a]	182[a]	[b]
free-standing h-BN film		100	182[a]	182[a]	[b]
h-BN/Ni(111)[c]	commensurate	91	170	170	[16]
h-BN/Pt(111)[c]	incommensurate	99	173	183	[16]
h-BN nanosheets[d]		101	170		[25]
bulk h-BN[e]		97, 103	169, 170	200	[28]

[a]Could not be resolved into separate TO$_\parallel$ and LO peaks. [b]This work. [c]HREELS of monolayer film grown in vacuum. [d]FTIR of chemically exfoliated sheets. [e]IR and Raman of bulk h-BN.

■ ACKNOWLEDGMENTS

■ REFERENCES

(1) Lindsay, L.; Broido, D. A. Enhanced Thermal Conductivity and Isotope Effect in Single-Layer Hexagonal Boron Nitride. *Phys. Rev. B: Condens. Matter Mater. Phys.* **2011**, *84*, 155421.

(2) Kim, K. K.; Hsu, A.; Jia, X.; Kim, S. M.; Shi, Y.; Hofmann, M.; Nezich, D.; Rodriguez-Nieva, J. F.; Dresselhaus, M.; Palacios, T.; et al. Synthesis of Monolayer Hexagonal Boron Nitride on Cu foil Using Chemical Vapor Deposition. *Nano Lett.* **2012**, *12*, 161−166.

(3) Yung, K. C.; Liem, H. Enhanced Thermal Conductivity of Boron Nitride Epoxy-Matrix Composite through Multi-Modal Particle Size Mixing. *J. Appl. Polym. Sci.* **2007**, *106*, 3587−3591.

(4) Jo, I.; Pettes, M. T.; Kim, J.; Watanabe, K.; Taniguchi, T.; Yao, Z.; Shi, L. Thermal Conductivity and Phonon Transport in Suspended Few-Layer Hexagonal Boron Nitride. *Nano Lett.* **2013**, *13*, 550−554.

(5) Wang, J.; Zhao, R.; Liu, Z.; Liu, Z. Widely Tunable Carrier Mobility of Boron Nitride-Embedded Graphene. *Small* **2013**, *9*, 1373−1378.

(6) Schiefele, J.; Sols, F.; Guinea, F. Temperature Dependence of the Conductivity of Graphene on Boron Nitride. *Phys. Rev. B: Condens. Matter Mater. Phys.* **2012**, *85*, 195420.

(7) Dai, S.; Fei, Z.; Ma, Q.; Rodin, A. S.; Wagner, M.; McLeod, A. S.; Liu, M. K.; Gannett, W.; Regan, W.; Watanabe, K.; et al. Tunable Phonon Polaritons in Atomically Thin van der Waals Crystals of Boron Nitride. *Science* **2014**, *343*, 1125−1129.

(8) Li, P.; Lewin, M.; Kretinin, A. V.; Caldwell, J. D.; Novoselov, K. S.; Taniguchi, T.; Watanabe, K.; Gaussmann, F.; Taubner, T. Hyperbolic Phonon-Polaritons in Boron Nitride for Near-Field Optical Imaging and Focusing. *Nat. Commun.* **2015**, *6*, 7507.

(9) Igami, M.; Fujita, M.; Mizuno, S. Phonon Dispersion of Nano-Graphite Ribbons. *Appl. Surf. Sci.* **1998**, *130−132*, 870−875.

(10) Wang, Y.; Qiu, B.; Ruan, X. Edge Effect on Thermal Transport in Graphene Nanoribbons: A Phonon Localization Mechanism Beyond Edge Roughness Scattering. *Appl. Phys. Lett.* **2012**, *101*, 013101.

(11) Akhoondali, H.; Goharrizi, A. Y.; Sharifi, M. J. Combined Effect of Edge Roughness and Phonon Scattering on the Electronic Properties of Ultra Scaled Graphene Nano-ribbons. *Superlattices Microstruct.* **2014**, *75*, 268−277.

(12) Gorbachev, R. V.; Riaz, I.; Nair, R. R.; Jalil, R.; Britnell, L.; Belle, B. D.; Hill, E. W.; Novoselov, K. S.; Watanabe, K.; Taniguchi, T.; et al. Hunting for Monolayer Boron Nitride: Optical and Raman Signatures. *Small* **2011**, *7*, 465−468.

(13) Lu, J.; Yeo, P. S. E.; Zheng, Y.; Xu, H.; Gan, C. K.; Sullivan, M. B.; Castro Neto, A. H.; Loh, K. P. Step Flow Versus Mosaic Film Growth in Hexagonal Boron Nitride. *J. Am. Chem. Soc.* **2013**, *135*, 2368−2373.

(14) Goriachko, A.; He; Knapp, M.; Over, H.; Corso, M.; Brugger, T.; Berner, S.; Osterwalder, J.; Greber, T. Self-Assembly of a Hexagonal Boron Nitride Nanomesh on Ru(0001). *Langmuir* **2007**, *23*, 2928−2931.

(15) Laskowski, R.; Blaha, P.; Schwarz, K. Bonding of Hexagonal BN to Transition Metal Surfaces: An ab initio Density-Functional Theory Study. *Phys. Rev. B: Condens. Matter Mater. Phys.* **2008**, *78*, 045409.

(16) Rokuta, E.; Hasegawa, Y.; Suzuki, K.; Gamou, Y.; Oshima, C.; Nagashima, A. Phonon Dispersion of an Epitaxial Monolayer Film of Hexagonal Boron Nitride on Ni(111). *Phys. Rev. Lett.* **1997**, *79*, 4609−4612.

(17) Simonson, R. J.; Paffett, M. T.; Jones, M. E.; Koel, B. E. A Vibrational Study of Borazine Adsorbed on Pt(111) and Au(111) Surfaces. *Surf. Sci.* **1991**, *254*, 29−44.

(18) Jin, C.; Lin, F.; Suenaga, K.; Iijima, S. Fabrication of a Freestanding Boron Nitride Single Layer and Its Defect Assignments. *Phys. Rev. Lett.* **2009**, *102*, 195505.

(19) Corso, M.; Auwärter, W.; Muntwiler, M.; Tamai, A.; Greber, T.; Osterwalder, J. Boron Nitride Nanomesh. *Science* **2004**, *35*, 217−220.

(20) Preobrajenski, A. B.; Nesterov, M. A.; Ng, M. L.; Vinogradov, A. S.; Mårtensson, N. Monolayer h-BN on Lattice-Mismatched Metal Surfaces: On the Formation of the Nanomesh. *Chem. Phys. Lett.* **2007**, *446*, 119−123.

(21) Ćavar, E.; Westerström, R.; Mikkelsen, A.; Lundgren, E.; Vinogradov, A. S.; Ng, M. L.; Preobrajenski, A. B.; Zakharov, A. A.; Mårtensson, N. A Single h-BN Layer on Pt(1 1 1). *Surf. Sci.* **2008**, *602*, 1722−1726.

(22) Tanaka, T.; Itoh, A.; Yamashita, K.; Rokuta, E.; Oshima, C. Heteroepitaxial System of h-BN/monolayer Graphene on Ni(111). *Surf. Rev. Lett.* **2003**, *10*, 697−703.

(23) Zhang, W. J.; Kanda, H.; Matsumoto, S. Cathodoluminescence of Cubic Boron Nitride Films Deposited by Chemical Vapor Deposition. *Appl. Phys. Lett.* **2002**, *81*, 3356−3358.

(24) Beghi, M. G.; Bottani, C. E.; Miotello, A.; Ossi, P. M. Vibrational Spectroscopy of Mixed Hexagonal-Cubic Boron Nitride Thin Films. *Thin Solid Films* **1997**, *308−309*, 107−112.

(25) Wang, Y.; Shi, Z.; Yin, J. Boron Nitride Nanosheets: Large-Scale Exfoliation in Methanesulfonic Acid and their Composites with Polybenzimidazole. *J. Mater. Chem.* **2011**, *21*, 11371−11377.

(26) Paduano, Q. S.; Snure, M.; Bondy, J.; Zens, T. W. C. Self-Terminating Growth in Hexagonal Boron Nitride by Metal Organic Chemical Vapor Deposition. *Appl. Phys. Express* **2014**, *7*, 071004.

(27) Shi, Y.; Hamsen, C.; Jia, X.; Kim, K. K.; Reina, A.; Hofmann, M.; Hsu, A. L.; Zhang, K.; Li, H.; Juang, Z.-Y.; et al. Synthesis of Few-Layer Hexagonal Boron Nitride Thin Film by Chemical Vapor Deposition. *Nano Lett.* **2010**, *10*, 4134−4139.

(28) Geick, R.; Perry, C. H.; Rupprecht, G. Normal Modes in Hexagonal Boron Nitride. *Phys. Rev.* **1966**, *146*, 543−547.